Published in final edited form as:
Biomaterials. 2010 September ; 31(25): 6425–6435. doi:10.1016/j.biomaterials.2010.04.064.

THE DIFFERENTIAL REGULATION OF CELL MOTILE ACTIVITY THROUGH MATRIX STIFFNESS AND POROSITY IN THREE DIMENSIONAL COLLAGEN MATRICES

Miguel Miron-Mendoza, **Joachim Seemann**, and **Frederick Grinnell***
Department of Cell Biology, University of Texas Southwestern Medical Center, 5323 Harry Hines Blvd. Dallas, Texas 75390-9039

Abstract

In three dimensional collagen matrices, cell motile activity results in collagen translocation, cell spreading and cell migration. Cells can penetrate into the matrix as well as spread and migrate along its surface. In the current studies, we quantitatively characterize collagen translocation, cell spreading and cell migration in relationship to collagen matrix stiffness and porosity. Collagen matrices prepared with 1 to 4 mg/ml collagen exhibited matrix stiffness (storage modulus measured by oscillating rheometry) increasing from 4 to 60 Pa and matrix porosity (measured by scanning electron microscopy) decreasing from 4 to 1 μm^2. Over this collagen concentration range, the consequences of cell motile activity changed markedly. As collagen concentration increased, cells no longer were able to cause translocation of collagen fibrils. Cell migration increased and cell spreading changed from dendritic to more flattened and polarized morphology depending on location of cells within or on the surface of the matrix. Collagen translocation appeared to depend primarily on matrix stiffness, whereas cell spreading and migration were less dependent on matrix stiffness and more dependent on collagen matrix porosity.

Keywords

Extracellular matrix; Matrix stiffness; Matrix porosity; Collagen translocation; Cell migration; Cell spreading; Mechanoregulation

INTRODUCTION

Fibrous connective tissues provide mechanical support and frameworks for the other tissues of the body. Type I collagen is the major protein component of fibrous connective tissues. Fibroblasts are the cell type primarily responsible for collagen biosynthesis and remodeling. Interactions between fibroblasts and the surrounding collagen matrix establish a homeostatic mechanism for tissues to respond to diverse mechanical forces including interstitial fluid flow [1], tissue stretch [2], and tissue loss [3,4]. Abnormal functioning of tissue mechanical homeostasis contributes to pathological changes in aging [5], fibrotic disease [6,7] and tumor progression [8,9].

*Corresponding author: Tel. 214 648–2181, frederick.grinnell@utsouthwestern.edu.

Three dimensional collagen matrix cultures exhibit structural and mechanical features that resemble fibrous connective tissue [10–12]. These matrices have been used to investigate cell physiology in a tissue-like environment [1,13–16]. On 2D culture surfaces, cell spreading and migration can be described in terms of a balance between cellular forces of protrusion, contraction, and adhesion [17,18]. The situation is more complicated in 3D matrices [19]. Matrix porosity makes possible entanglement between the cells and matrix fibrils, and initial cell spreading is typically dendritic [15]. Cells exhibit dual modes of migration -- mesenchymal and amoeboid [20,21]. In mesenchymal migration, the cells attach to and pull on the matrix. In amoeboid migration, cells protrude through the spaces and push off the matrix. In addition, cells in 3D matrices can remodel matrix topography to produce their own migratory tracks [22–24].

Recently, we reported that fibroblast migration and collagen translocation were coupled in 3D collagen matrices. The balance between the two appeared to depend on how well the matrix resisted tractional force exerted by fibroblasts [25]. The features of matrix biomechanics that regulate cell physiological response are poorly understood. In the current work, we investigate quantitatively the effects of matrix stiffness and porosity on collagen translocation, cell spreading and cell migration

MATERIALS AND METHODS

Materials

Type I rat tail collagen high concentration was purchased from BD Biosciences (Bedford, MA). Dulbecco's modified Eagle medium (DMEM), CO_2-independent DMEM and 0.25% trypsin/EDTA solution were purchased from Invitrogen (Gaithersburg, MD). Fetal bovine serum (FBS) was purchased from Atlanta Biologicals (Lawrenceville, GA). Platelet-derived growth factor BB isotype (PDGF) was obtained from Upstate Biotechnology, Inc. (Lake Placid, NY). Fatty acid-free bovine serum albumin (BSA), Sodium borohydride, and Collagenase A were obtained from Sigma (St. Louis, MO). Alexa Fluor 594 phalloidin and Propidium Iodine (PI) were obtained from Molecular Probes, Inc. (Eugene, OR). RNase (DNase free) was purchased from Roche (Indianapolis, IN). Anti-actin and anti-vinculin antibodies were obtained from Sigma (St. Luis MO). Antibodies to focal adhesion kinase (FAK) were purchased from BD Transduction Laboratories (Franklin Lakes, NJ). Antibodies to phosphor (Y397) FAK were purchased from Biosource International (Camarillo CA). Goat-anti-mouse HP-conjugated was obtained from ICN Biomedicals (Aurora, OH). Goat-anti-rabbit HP-conjugated was purchased from Thermo Fisher Scientific (Rockford, IL). 6 μm Fluoresbrite YG Microspheres were obtained from Polysciences. Inc. (Warrington, PA). Fluoromount G was obtained from Southern Biotechnology Associates (Birmingham, AL).

Cell culture

Use of human foreskin fibroblasts was approved by the University Institutional Review Board (Exemption #4). BR5 human foreskin fibroblasts [26] were cultured in DMEM supplemented with 10% FCS. Cell culture was carried out at 37°C in a 5% CO_2 humidified incubator. Experiments were carried out in DMEM (or CO_2-independent DMEM for time-lapse studies) containing 5 mg/ml BSA and 50 ng/ml PDGF.

Cell migration and collagen translocation in nested collagen matrices

Preparation of restrained and floating nested collagen matrices and measurement of cell migration and collagen translocation in nested matrices were accomplished as before [25]. Briefly, dermal equivalents were formed by overnight contraction of 200 μl collagen matrices (1.5 mg/ml collagen, 2×10^5 cells/matrix). Subsequently, dermal equivalents were embedded in 200 μl outer cell-free collagen matrices with collagen concentration in outer matrices ranging

from 1 to 4 mg/ml as indicated in the figure legends. A layer of outer matrix underneath the inner matrix prevents any direct interactions between the cells and culture surface. To obtain floating nested matrices, samples were gently released from the culture dishes after 1h polymerization. Restrained and floating nested matrix cultures were incubated 24 h in PDGF-containing medium. *Cell Migration Index* was determined using propidium iodide-stained samples by counting the average number of cells that migrated out of dermal equivalents in four 10X microscopic fields selected arbitrarily. Each field included the border of the dermal equivalent (detected by dark field microscopy) and the furthest moving cells. In some experiments, 6 μm fluorescent microspheres were added (1:200) to the outer matrices. Collagen translocation was quantified using the *Analyze Particle Function* of Image J software by measuring bead accumulation at the interface between inner and outer matrices relative to starting conditions.

3D reconstruction of cell migration in nested matrices was carried out using Imaris software (version 5.0 from Bitplane AG). Z stacks images were collected with a Leica TCS SP1 confocal microscope using a 20X/0.75 HC PL APO objective from Leica. Z stack images were taken in steps of 2 μm and usually covered a range of 100 μm from the first cell visualized on the top of the matrix to the last cell visualized in the bottom of the matrix.

Cell spreading, migration and collagen translocation in uniform collagen matrices

For time-lapse analysis of fibroblasts within collagen matrices, neutralized collagen solutions (1 to 4 mg/ml, 200 mu;l) containing cells (10^3/matrix) were polymerized 1 h and then incubated 4 h in PDGF-containing medium. For time-lapse analysis of fibroblasts on the surface of collagen matrices, matrices were polymerized 1 h after which cells were added and then incubated 4 h. Time-lapse analysis of uniform matrices was accomplished using a Zeiss Axiovert 200M inverted microscope equipped with an A-PLAN 10X/0.25 PH1 Zeiss objective and a Hamamatsu Model Orca 285 CCD camera. Images were acquired at 5 min intervals using Openlab 4.02 (Improvision) software. Collagen translocation was analyzed by measuring the displacement of 6 μm beads (eight/sample) embedded in the matrices. Samples to be analyzed by Immunostaining were prepared as above but contained 10^4 cells/matrix.

To increase matrix stiffness chemically, polymerized matrices were treated with 0.5% glutaraldehyde for 2 h at room temperature. Subsequently, samples were rinsed twice (5 min) with phosphate buffered saline (PBS) followed by 2 × 2 h incubations in 2% glycine in PBS, 2 × 30 min incubations in 1% sodium borohydride in H_20, overnight incubation with 2% glycine in PBS, rinsed twice with PBS, and finally incubated 1 h with DMEM at 37°C. Control matrices were treated identically except with PBS substituted for glutaraldehyde treatment. Time-lapse and immunostaining analyses of cells on the surfaces of glutaraldehyde-treated matrices were carried out as above.

Immunostaining

Immunostaining of fixed and permeabilized cells was accomplished as described previously using Alexa fluor-594 phalloidin to detect for actin, propidium iodide to detect cell nuclei, and anti-vinculin antibodies to detect focal adhesions [26,27]. Samples were mounted on glass slides with Fluoromount G (Southern Biotechnology Associates, Birmingham, AL). Images were collected with a Nikon Eclipse E600 fluorescence microscope and 10X/0.45 and 20X/0.75 Nikon Plan Apo infinity corrected objectives using a Photometrics SenSys CCD camera and MetaVue imaging software (Molecular Devices). Morphometric measurements were carried out using MetaVue software. Dendritic Cell Index -- cell perimeter^2/4π· area (1.0 for a round cell) – was determined using the *Integrated Morphometry Analysis* function. Data presented for each condition are based on measurement of five cells in three separate experiments.

Immunoblotting

Immunoblotting was accomplished as described previously [26] except that cell lysates were treated with collagenase (10 U/gel) for 10 min at 37° C before adding SDS-PAGE sample buffer. Blots were probed with mouse anti-actin, mouse anti-FAK, and rabbit anti-pFAK antibodies followed by HP-conjugated goat- anti-mouse and anti-rabbit. Without pretreatment of the samples with collagenase, it was difficult to visualize FAK and phospho-FAK in the samples.

Scanning Electron Microscopy and Matrix Porosity

Collagen matrices were polymerized and prepared for scanning electron microscopy (SEM) using a combination of glutaraldehyde and osmium fixation followed by critical-pointed drying and paladium coating as described previously [26]. SEM specimens were analyzed and photographed with a 840A scanning electron microscope (JEOL, Tokyo, Japan). SEM images were subjected to thresholding to convert matrix pores and collagen fibrils to black and white images, adjusting pixel density so that obviously deep collagen fibrils were eliminated. The 2D black and white representation of the matrix was evaluated using the analyze particle function of Image J (particles = black pores) with 100 nm set as the lower limit.

Rheometry

Collagen matrices was measured by oscillation rheometry using an AR-G2 rheometer (TA instruments, New Castle, DE) with parallel plate geometry. 12 mm diameter collagen samples were polymerized in special designed plates that later were mounted to be the base plate of the rheometer. Subsequently a 12 mm diameter plate was lowered onto the sample until filling the gap between both plates. Measurements were carried out in a controlled 21 °C room temperature. To characterize matrix response for the first time, the shear modulus was measured using oscillatory strain and strain sweep at a frequency of 0.1 Hz until sample breaks. Once the linear response of matrices was found, subsequent measurements were performed with an oscillating fixed 0. 5% strain amplitude and at a frequency of 0.1 Hz for 30 min. Storage (G′) modulus was registered for each sample. Data presented for each condition are based on measurement of three samples in two separate experiments

RESULTS

Cell migration and collagen translocation in nested collagen matrices prepared with 1 to 4 mg/ml collagen outer matrices

In nested collagen matrices, fibroblasts migrate out of a cell-containing inner matrix (IM) into a cell-free, outer matrix (OM). Nested matrices can be restrained on an underlying culture dish or floating in medium (Figures 1A and 1B). We compared cell migration in floating and restrained nested matrices as a function of collagen concentration in the outer matrix. Figure 1C shows that in floating nested matrices with 1 mg/ml outer matrices, little cell migration occurred. However, as the collagen concentration in the outer matrix was increased, cell migration increased. With 2 mg/ml collagen in the outer matrix, cell migration in floating nested matrices was equivalent to that observed if the nested matrices were restrained.

Although the extent of cell migration in restrained nested matrices did not change between 1 to 4 mg/ml collagen, the pattern of migration varied. This variation can be observed in Figure 1B, which shows top and side 3D reconstruction views of the distribution of migrating cells (entire depth of field = ~100 μm). With 1.5 mg/ml outer matrices, the density of migrating cells was higher in regions closer to the underlying culture surface on which the nested matrices were restrained. However, if the concentration of collagen in the outer matrix was increased to 4 mg/ml, then the distribution of migrating cells was more uniform. Time lapse time-lapse

videos demonstrated that the trajectory of cell migration was oriented towards the restraining surface with 1.5 mg/ml but not 4 mg/ml outer matrices.

Previously, we showed that collagen translocation was favored over cell migration if nested matrices are were floating rather than restrained [25]. Figure 2 describes experiments with floating nested matrices to measure the dependence of collagen translocation on outer matrix collagen concentration. Collagen translocation was assessed by observing movement of 6 μm fluorescent beads trapped within the outer matrix. Accumulation of beads at the interface between outer and inner matrices was highest with 1 mg/ml outer matrices and decreased as the collagen concentration was increased (Figure 2A). Quantification of bead accumulation relative to the starting distribution showed a progressive decline from a 6 fold increase in bead accumulation with 1 mg/ml outer matrices to no detectable increase with 4 mg/ml outer matrices (Figure 2B).

Quantitative measurements on the porosity and stiffness of collagen matrices varying from 1 to 4 mg/ml collagen

Taken together, the findings in Figures 1 and 2 show that the consequences of cell motile activity in nested collagen matrices changed dramatically when the collagen concentration in the outer matrix was increased from 1 to 4 mg/ml. As the collagen density increased, collagen translocation decreased. At higher collagen concentrations, cell migration became independent of the underlying restraining surface. Independence was shown by the increased extent of cell migration in floating nested matrices and the altered trajectory of cell migration in restrained nested matrices.

Experiments were carried out to determine porosity and stiffness of collagen matrices varying from 1 to 4 mg/ml. Figure 3A shows the appearance of collagen matrices ranging from 1 to 4 mg/ml visualized by scanning electron microscopy. To quantify matrix porosity, SEM images were subjected to thresholding using a 0.1 μm lower limit, and average void space between collagen fibers was determined. Figure 3B shows that over the range of 1 to 4 mg/ml, the average pore area decreased from 3.7 μm^2 to 0.9 μm^2, which corresponds to average pore diameter ranging from 2.2 to 1.1 μm. We also measured stiffness (storage modulus) of the matrices using an oscillating rheometer. Figure 3C shows that as collagen concentration increased from 1 to 4 mg/ml, matrix stiffness increased from 4 to 62 Pa.

Motile activity of fibroblasts within and on top of collagen matrices

The inner component of nested collagen matrices (Figure 1A) is prepared by overnight contraction of a floating collagen matrix. Volume decreases approximately 90% with no loss off collagen. As a result, the collagen concentration increases from ~1.5 mg/ml to ~15 mg/ml, and the storage modulus overnight contracted matrices was measured to be 855 +/− 93 Pa (SEM?). Therefore, fibroblasts migrating in nested matrices cross an interface changing in stiffness by more than an order of magnitude.

One interpretation of the findings in Figures 1 and 2 was that the outer matrix collagen concentration-dependence of collagen translocation and cell migration were responses to mechanical restraints imposed by the interface. On the other hand, collagen-dependence of collagen translocation and cell migration may have reflected coupling between fibroblast motile activity and matrix mechanical features independent of the interface. Therefore, we also measured individual cell motile behavior using fibroblasts sparsely distributed either within and on the surfaces of uniform collagen matrices.

Figures 4A and 4B present phase-contrast images from time-lapse videos of fibroblasts incubated for 4 h within (Supplemental time-lapse videos 1 and 2) and on the surfaces

(Supplemental time-lapse videos 3 and 4) of 1 and 4 mg/ml collagen matrices. Regardless whether cells were within or on the surfaces of the matrices, collagen fibrils translocated towards the cells in 1 mg/ml matrices and remained stationary in 4 mg/ml matrices. Figure 5A shows quantification of collagen translocation towards the cells based on displacement of 6 μm beads trapped within the matrices. The extent of collagen translocation (Bead Trans.) decreased with increasing collagen concentration over the range of 1–4 mg/ml.

During the 4 h incubation period, cell spreading occurred. Spreading of cells within or on the surfaces of 1 mg/ml matrices was dendritic. However, spreading of fibroblasts within 4 mg/ml matrices was dendritic whereas cells became flattened and polarized if they were located on the matrix surface.

Parallel experiments were carried out with fixed and stained cultures (cf. Figure 6A). Figures 5B and 5C show morphometric measurements of fibroblast spreading (projected cell area) and overall cell shape (dendritic index = 1 for a round cell). Over the collagen concentration range of 1 to 4 mg/ml, the extent of cell spreading increased about 50%. In general, fibroblasts within or on the surfaces of matrices showed somewhat greater spreading as the collagen concentration increased. However, the biggest difference was in cell shape as had been observed in the time-lapse videos. That is, dendritic index was similar for cells within matrices or on the surfaces of 1–2 mg/ml matrices. Above 2 mg/ml, dendritic index remained relatively constant for cells within matrices but decreased for fibroblasts on the matrix surfaces.

Actin stress fibers, focal adhesions, and focal adhesion kinase (FAK, Y397) phosphorylation

Figure 6A shows the collagen concentration-dependent transition in morphology from dendritic to flattened and polarized of fibroblasts on the surfaces of the matrices. Actin stress fibers (phalloidin-staining) were readily visible in the flattened cell regions. Focal adhesion could be observed by immunostaining for vinculin. To test functionality of focal adhesions, we measured FAK (Y397) phosphorylation. Figure 6B shows that for cells on collagen-coated coverslips (2D), robust FAK phosphorylation could be observed after 1 hr, whereas little FAK phosphorylation was detected at this time in fibroblasts interacting with 1 and 4 mg/ml collagen matrices (M1 & M4) or trypsinized cells (T). However, after 4 h, FAK phosphorylation also could be detected in fibroblasts interacting with 1 and 4 mg/ml collagen matrices.

Cell spreading and migration on glutaraldehyde-treated collagen matrices

The collagen concentration-dependent transition in morphology of fibroblasts on the surfaces of collagen matrices might have occurred because of increased matrix stiffness. To test this possibility, matrices were stiffened by treatment with glutaraldehyde. Figure 7A shows storage modulus vs. collagen concentration for glutaraldehyde-treated (glu-treated) and control matrices. The results are presented on a logarithmic scale to facilitate comparison. Glutaraldehyde treatment increased matrix stiffness as much as 10 fold. Glu-treated 1.75 mg/ml collagen matrices exhibited a storage modulus similar to 4 mg/ml control matrices.

Motile activity of fibroblasts was compared on control and glu-treated matrices. Figures 7B and 7C present morphometric measurements of fibroblast spreading and dendritic index, and Figure 8 shows the appearance of phalloidin-stained cells. Cell morphology and quantitative measures of fibroblast spreading and dendritic index showed similar collagen concentration dependence over the range of 1 to 4 mg/ml collagen matrices regardless whether or not the matrices had been glu-treated.

Finally, Figure 9A shows phase-contrast images from representative time-lapse videos of fibroblasts on the surfaces of fixed 1 and 4 mg/ml collagen matrices (Supplemental time-lapse videos 5 and 6). In contrast to control matrices (Figures 4 and 5A), little collagen translocation

occurred in 1 or 4 mg/ml matrices that were glu-treated. However, fibroblasts on 4 mg/ml but not 1 mg/ml glu-treated matrices began to migrate. Figure 9B shows quantitative data on the extent of cell migration (nuclear displacement). Cell migration was similar on control and glu-treated matrices.

DISCUSSION

The features of matrix biomechanics that regulate cell physiological responses are poorly understood. We found that over the collagen concentration range of 1 to 4 mg/ml, the consequences of fibroblast motile activity changed markedly. Collagen fibril translocation decreased and cell spreading and migration increased depending on location of cells within or on the surface of the matrix. As will be discussed, collagen translocation appeared to depend primarily on matrix stiffness, whereas fibroblast spreading and migration were influenced strongly by collagen matrix porosity.

Increasing the collagen concentration of matrices from 1 to 4 mg/ml resulted in an increase in matrix stiffness from 4 to 62 Pa (storage modulus) as measured by an oscillating rheometer. Stiffness measurements were made at low strain (0.5%) and frequency (0.1 Hz). Although collagen matrices have been shown to exhibit linearity up to 10% strain [28], atypical behavior has been reported at low collagen matrix concentrations [29]. We used low strain and frequency to insure a linear response over the range of collagen concentrations that we tested, and our results are similar to those reported by others using rheological methods [28–31]. In the experiments using glutaraldehyde treatment to increase matrix stiffness, glycine and Na borohydride treatments were included to prevent cytotoxic effects of glutaraldehyde [32,33], and fibroblasts interacting with glutaraldehyde-treated matrices did not show evidence of morphological abnormalities.

Increasing the collagen concentration from 1 to 4 mg/ml also resulted in a decrease in matrix porosity from 3.7 μm^2 to 0.9 μm^2 -- corresponding to average pore diameter 2.2 to 1.1 μm. Since preparation of the samples for scanning electron microscopy analysis involved a combination of glutaraldehyde and osmium fixation followed by critical-pointed drying and paladium coating, the data likely reflect relative rather than absolute pore sizes. Nevertheless, our findings are in the same size range as reported for native collagen matrices analyzed by 3D reconstruction confocal reflection microscopy [34].

As the collagen concentration in the outer matrix of floating nested matrices was increased from 1 to 4 mg/ml, the ability of cell motile activity to cause collagen translocation decreased, and little collagen translocation occurred with 4 mg/ml outer matrices. Similarly, fibroblasts spreading within or on the surfaces of uniform collagen matrices showed decreased collagen translocation as collagen concentration increased from 1 to 4 mg/ml. After matrix stiffening with glutaraldehyde, translocation of 1 mg/ml collagen matrices no longer occurred. Taken together, these findings suggested that matrix stiffness determined the possibility of collagen translocation independently of cell population or position.

In contrast to collagen translocation, the effects of collagen concentration on cell migration and spreading varied according to cell population and position within the matrix indicating that collagen concentration influenced cell migration and spreading by mechanisms different from collagen translocation. For instance, with floating nested collagen matrices, increasing the collagen concentration from 1 to 2 mg/ml was sufficient for maximal cell migration. On the other hand, differences in spreading and migration of fibroblasts in uniform collagen matrices were not observed in 2 mg/ml collagen matrices, but did become evidence at higher collagen concentrations. Above 2 mg/ml collagen, cells on the surfaces but not within collagen matrices switched from dendritic to flattened and polarized morphology and exhibited migration.

Studies comparing control and glutaraldehyde-treated collagen matrices provided direct evidence that matrix stiffness was not responsible for the switch from dendritic morphology to flattened, polarized and migratory that occurred when fibroblasts were incubated on the surfaces of high concentration collagen matrices. That is, increasing matrix stiffness 3–10 fold by glutaraldehyde treatment had no effect on cell spreading and migration. Surface topography [35] and arrangement of adhesion ligand domains [36–38] have been shown to exert a strong influence on cell morphology and migration on 2D surfaces. Our findings support the idea that closer spacing of collagen fibrils (i.e., decreased matrix porosity) plays a key regulatory role in determining cell spreading and migration in collagen matrices.

To test signaling function of focal adhesions formed by fibroblast on the surfaces of collagen matrices, we measured activation of focal adhesion kinase (FAK), which plays a key role in cell motile function [39]. Most studies on cells interacting with 3D matrices have demonstrated absence of FAK signaling as measured by FAK (Y397) phosphorylation [40–42]. Consistent with previous findings, we also observed a lack of FAK phosphorylation after short incubation periods. However, slow FAK (Y397) phosphorylation occurred and could be detected after 4 h. The biological significance and regulatory mechanism of slow FAK phosphorylation require further investigation.

The collagen-concentration dependent behavior that we observed for fibroblasts interacting with collagen matrices differs markedly from the results of studies on 2D surface biomechanics using ligand-coated polyacrylamide surfaces. The softest polyacrylamide surfaces have stiffness values in the range of 200–1000 Pa [43], and are stiffer than 1–4 mg/ml collagen matrices. Yet, fibroblasts on soft polyacrylamide surfaces tend to remain round and spread poorly [43–45], migrate poorly [Pelham, 1997 #141;Lo, 2000 #287;] and form cell clusters [46].

The difference between our studies on 3D collagen matrices and previous findings with 2D polyacrylamide surfaces may derive in part because of the growth factor environment. The studies with polyacrylamide surfaces were carried out in serum-containing medium, whereas we used medium containing PDGF, which stimulates fibroblast migration in 3D matrices more than other growth factors that we have tested [47]. Indeed, human fibroblasts incubated on the surfaces of 1 to 4 mg/ml collagen matrices in serum-containing medium spread much more slowly that in PDGF-containing medium and contract into clusters rather than migrating as individuals [48]. We speculate that in serum-contain medium, because of the contractile effect of Rho activation [49], fibroblasts require a stiff surface against which to pull in order to overcome the forces of cell membrane tension and tensegrity that tend to impede cell polarization [50,51]. On the other hand, PDGF-stimulated Rac activation [52] facilitates cell protrusion and dendritic morphology [4,15]. Understanding the differences in cell behavior on 3D collagen matrices vs. 2D polyacrylamide surfaces is an important topic for future investigation.

CONCLUSIONS

In the current studies, we quantitatively characterize collagen translocation, cell spreading and cell migration in collagen matrices varying in collagen concentration. Collagen translocation appeared to depend primarily on collagen matrix stiffness, whereas cell spreading and migration were less dependent on matrix stiffness and more dependent on collagen matrix porosity.

Supplementary Material

Refer to Web version on PubMed Central for supplementary material.

Acknowledgments

This research was supported by grants from the National Institutes of Health, GM31321 (to FG) and the UT Southwestern Endowed Scholars Program (to JS). We are indebted to Drs. William Snell and Matt Petroll for their helpful advice.

References

1. Pedersen JA, Boschetti F, Swartz MA. Effects of extracellular fiber architecture on cell membrane shear stress in a 3D fibrous matrix. J Biomech 2007;40:1484–92. [PubMed: 16987520]
2. Langevin HM, Bouffard NA, Badger GJ, Iatridis JC, Howe AK. Dynamic fibroblast cytoskeletal response to subcutaneous tissue stretch ex vivo and in vivo. Am J Physiol Cell Physiol 2005;288:C747–56. [PubMed: 15496476]
3. Tomasek JJ, Gabbiani G, Hinz B, Chaponnier C, Brown RA. Myofibroblasts and mechano-regulation of connective tissue remodelling. Nat Rev Mol Cell Biol 2002;3:349–63. [PubMed: 11988769]
4. Grinnell F. Fibroblast biology in three-dimensional collagen matrices. Trends Cell Biol 2003;13:264–9. [PubMed: 12742170]
5. Fisher GJ, Varani J, Voorhees JJ. Looking older: fibroblast collapse and therapeutic implications. Arch Dermatol 2008;144:666–72. [PubMed: 18490597]
6. Desmouliere A, Darby IA, Gabbiani G. Normal and pathologic soft tissue remodeling: role of the myofibroblast, with special emphasis on liver and kidney fibrosis. Lab Invest 2003;83:1689–707. [PubMed: 14691287]
7. Abraham DJ, Eckes B, Rajkumar V, Krieg T. New developments in fibroblast and myofibroblast biology: implications for fibrosis and scleroderma. Curr Rheumatol Rep 2007;9:136–43. [PubMed: 17502044]
8. Weigelt B, Bissell MJ. Unraveling the microenvironmental influences on the normal mammary gland and breast cancer. Semin Cancer Biol 2008;18:311–21. [PubMed: 18455428]
9. Butcher DT, Alliston T, Weaver VM. A tense situation: forcing tumour progression. Nat Rev Cancer 2009;9:108–22. [PubMed: 19165226]
10. Silver FH, Siperko LM, Seehra GP. Mechanobiology of force transduction in dermal tissue. Skin Research Technol 2002;8:1–21.
11. Chandran PL, Barocas VH. Affine versus non-affine fibril kinematics in collagen networks: theoretical studies of network behavior. J Biomech Eng 2006;128:259–70. [PubMed: 16524339]
12. Ahlfors JE, Billiar KL. Biomechanical and biochemical characteristics of a human fibroblast-produced and remodeled matrix. Biomaterials 2007;28:2183–91. [PubMed: 17280714]
13. Barocas VH, Tranquillo RT. An anisotropic biphasic theory of tissue-equivalent mechanics: the interplay among cell traction, fibrillar network deformation, fibril alignment, and cell contact guidance. J Biomech Eng 1997;119:137–45. [PubMed: 9168388]
14. Brown RA, Prajapati R, McGrouther DA, Yannas IV, Eastwood M. Tensional homeostasis in dermal fibroblasts: mechanical responses to mechanical loading in three-dimensional substrates. J Cell Physiol 1998;175:323–32. [PubMed: 9572477]
15. Rhee S, Grinnell F. Fibroblast mechanics in 3D collagen matrices. Adv Drug Deliv Rev 2007;59:1299–1305. [PubMed: 17825456]
16. Yamada KM, Cukierman E. Modeling tissue morphogenesis and cancer in 3D. Cell 2007;130:601–10. [PubMed: 17719539]
17. Lauffenburger DA, Horwitz AF. Cell migration: a physically integrated molecular process. Cell 1996;84:359–69. [PubMed: 8608589]
18. Sheetz MP, Felsenfeld D, Galbraith CG, Choquet D. Cell migration as a five-step cycle. Biochem Soc Symp 1999;65:233–43. [PubMed: 10320942]
19. Friedl P, Wolf K. Plasticity of cell migration: a multiscale tuning model. J Cell Biol 2010;188:11–19. [PubMed: 19951899]
20. Friedl P, Brocker EB. The biology of cell locomotion within three-dimensional extracellular matrix. Cell Mol Life Sci 2000;57:41–64. [PubMed: 10949580]

21. Sanz-Moreno V, Gadea G, Ahn J, Paterson H, Marra P, Pinner S, et al. Rac activation and inactivation control plasticity of tumor cell movement. Cell 2008;135:510–23. [PubMed: 18984162]
22. Stopak D, Harris AK. Connective tissue morphogenesis by fibroblast traction. I. Tissue culture observations. Dev Biol 1982;90:383–98. [PubMed: 7075867]
23. Friedl P, Maaser K, Klein CE, Niggemann B, Krohne G, Zanker KS. Migration of highly aggressive MV3 melanoma cells in 3-dimensional collagen lattices results in local matrix reorganization and shedding of alpha2 and beta1 integrins and CD44. Cancer Res 1997;57:2061–70. [PubMed: 9158006]
24. Tranquillo RT. Self-organization of tissue-equivalents: the nature and role of contact guidance. Biochem Soc Symp 1999;65:27–42. [PubMed: 10320931]
25. Miron-Mendoza M, Seemann J, Grinnell F. Collagen Fibril Flow and Tissue Translocation Coupled to Fibroblast Migration in 3D Collagen Matrices. Mol Biol Cell 2008;19:2051–2058. [PubMed: 18321993]
26. Rhee S, Jiang H, Ho CH, Grinnell F. Microtubule function in fibroblast spreading is modulated according to the tension state of cell-matrix interactions. Proc Natl Acad Sci U S A 2007;104:5425–30. [PubMed: 17369366]
27. Tamariz E, Grinnell F. Modulation of fibroblast morphology and adhesion during collagen matrix remodeling. Mol Biol Cell 2002;13:3915–3929. [PubMed: 12429835]
28. Barocas VH, Moon AG, Tranquillo RT. The fibroblast-populated collagen microsphere assay of cell traction force--Part 2: Measurement of the cell traction parameter. J Biomech Eng 1995;117:161–70. [PubMed: 7666653]
29. Velegol D, Lanni F. Cell traction forces on soft biomaterials. I. Microrheology of type I collagen gels. Biophys J 2001;81:1786–92. [PubMed: 11509388]
30. Leung LY, Tian D, Brangwynne CP, Weitz DA, Tschumperlin DJ. A new microrheometric approach reveals individual and cooperative roles for TGF-beta1 and IL-1beta in fibroblast-mediated stiffening of collagen gels. FASEB J 2007;21:2064–73. [PubMed: 17341683]
31. Vader D, Kabla A, Weitz D, Mahadevan L. Strain-induced alignment in collagen gels. PLoS One 2009;4:e5902. [PubMed: 19529768]
32. Hey KB, Lachs CM, Raxworthy MJ, Wood EJ. Crosslinked fibrous collagen for use as a dermal implant: control of the cytotoxic effects of glutaraldehyde and dimethylsuberimidate. Biotechnol Appl Biochem 1990;12:85–93. [PubMed: 2106902]
33. Lee CR, Grodzinsky AJ, Spector M. The effects of cross-linking of collagen-glycosaminoglycan scaffolds on compressive stiffness, chondrocyte-mediated contraction, proliferation and biosynthesis. Biomaterials 2001;22:3145–54. [PubMed: 11603587]
34. Wolf K, Alexander S, Schacht V, Coussens LM, von Andrian UH, van Rheenen J, et al. Collagen-based cell migration models in vitro and in vivo. Semin Cell Dev Biol 2009;20:931–41. [PubMed: 19682592]
35. Curtis A, Wilkinson C. Topographical control of cells. Biomaterials 1997;18:1573–83. [PubMed: 9613804]
36. Beningo KA, Dembo M, Wang YL. Responses of fibroblasts to anchorage of dorsal extracellular matrix receptors. Proc Natl Acad Sci U S A 2004;101:18024–9. [PubMed: 15601776]
37. Zimerman B, Arnold M, Ulmer J, Blummel J, Besser A, Spatz JP, et al. Formation of focal adhesion-stress fibre complexes coordinated by adhesive and non-adhesive surface domains. IEE Proc Nanobiotechnol 2004;151:62–66. [PubMed: 16475844]
38. Doyle AD, Wang FW, Matsumoto K, Yamada KM. One-dimensional topography underlies three-dimensional fibrillar cell migration. J Cell Biol 2009;184:481–90. [PubMed: 19221195]
39. Mitra SK, Hanson DA, Schlaepfer DD. Focal adhesion kinase: in command and control of cell motility. Nat Rev Mol Cell Biol 2005;6:56–68. [PubMed: 15688067]
40. Cukierman E, Pankov R, Stevens DR, Yamada KM. Taking cell-matrix adhesions to the third dimension. Science 2001;294:1708–12. [PubMed: 11721053]
41. Wozniak MA, Desai R, Solski PA, Der CJ, Keely PJ. ROCK-generated contractility regulates breast epithelial cell differentiation in response to the physical properties of a three-dimensional collagen matrix. J Cell Biol 2003;163:583–95. [PubMed: 14610060]
42. Wei WC, Lin HH, Shen MR, Tang MJ. Mechanosensing machinery for cells under low substratum rigidity. Am J Physiol Cell Physiol 2008;295:C1579–89. [PubMed: 18923058]

43. Engler A, Bacakova L, Newman C, Hategan A, Griffin M, Discher D. Substrate compliance versus ligand density in cell on gel responses. Biophys J 2004;86:617–28. [PubMed: 14695306]
44. Yeung T, Georges PC, Flanagan LA, Marg B, Ortiz M, Funaki M, et al. Effects of substrate stiffness on cell morphology, cytoskeletal structure, and adhesion. Cell Motil Cytoskeleton 2005;60:24–34. [PubMed: 15573414]
45. Solon J, Levental I, Sengupta K, Georges PC, Janmey PA. Fibroblast adaptation and stiffness matching to soft elastic substrates. Biophys J 2007;93:4453–61. [PubMed: 18045965]
46. Guo WH, Frey MT, Burnham NA, Wang YL. Substrate rigidity regulates the formation and maintenance of tissues. Biophys J 2006;90:2213–20. [PubMed: 16387786]
47. Jiang H, Rhee S, Ho C-H, Grinnell F. Distinguishing fibroblast promigratory and procontractile growth factor environments in 3D collagen matrices. FASEB J 2008;22:2151–2160. [PubMed: 18272655]
48. Rhee S, Ho CH, Grinnell F. Promigratory and procontractile growth factor environments differentially regulate cell morphogenesis. Exp Cell Res 2010;316:232–244. [PubMed: 19796636]
49. Ridley AJ, Hall A. The small GTP-binding protein Rho regulates the assembly of focal adhesions and actin stress fibers in response to growth factors. Cell 1992;70:389–99. [PubMed: 1643657]
50. Ingber DE. Tensegrity: The architectural basis of cellular mechanotransduction. Annu Rev Physiol 1997;59:575–99. [PubMed: 9074778]
51. Sheetz MP, Dai J. Modulation of membrane dynamics and cell motility by membrane tension. Trends Cell Biol 1996;6:85–9. [PubMed: 15157483]
52. Ridley AJ, Paterson HF, Johnston CL, Diekmann D, Hall A. The small GTP-binding protein Rac regulates growth factor-induced membrane ruffling. Cell 1992;70:401–10. [PubMed: 1643658]

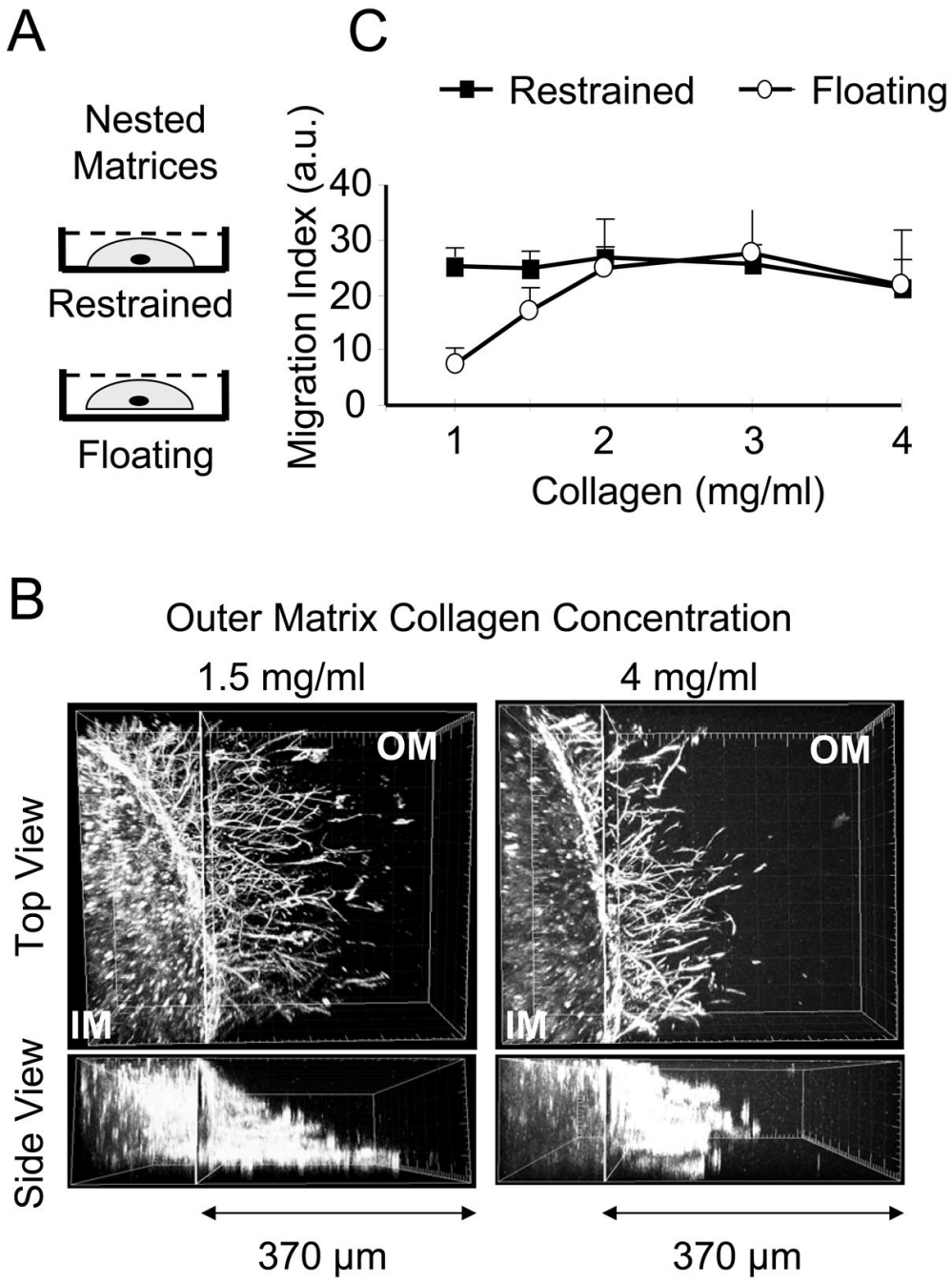

Figure 1. Fibroblast migration in nested collagen matrices prepared with 1 to 4 mg/ml collagen outer matrices

(A) Diagram of nested collagen matrices showing cell containing inner matrix within cell free outer matrix and nested matrices restrained on culture dishes or floating in medium. (B) Restrained nested matrices were incubated 24 h. 3D reconstruction shows pattern of cell migration from the inner matrix (IM) to the outer matrix (OM) with 1.5 and 4 mg/ml outer collagen concentrations. With 1.5 mg/ml outer matrices, the density of migrating cells was higher in regions closer to the underlying culture surface. If the concentration of collagen in the outer matrix was increased to 4 mg/ml, then the distribution of migrating cells was more uniform. (C) Restrained and floating nested matrices were prepared using the outer collagen

concentrations indicated and incubated 24 h after which cell migration index was determined. Data shown are the averages +/− SD of cell migration index based on three separate experiments with duplicate matrices at each collagen concentration. In floating nested matrices, cell migration index increased as the outer collagen concentration increased. In restrained nested matrices, cell migration index was similar over the range of outer collagen concentrations tested.

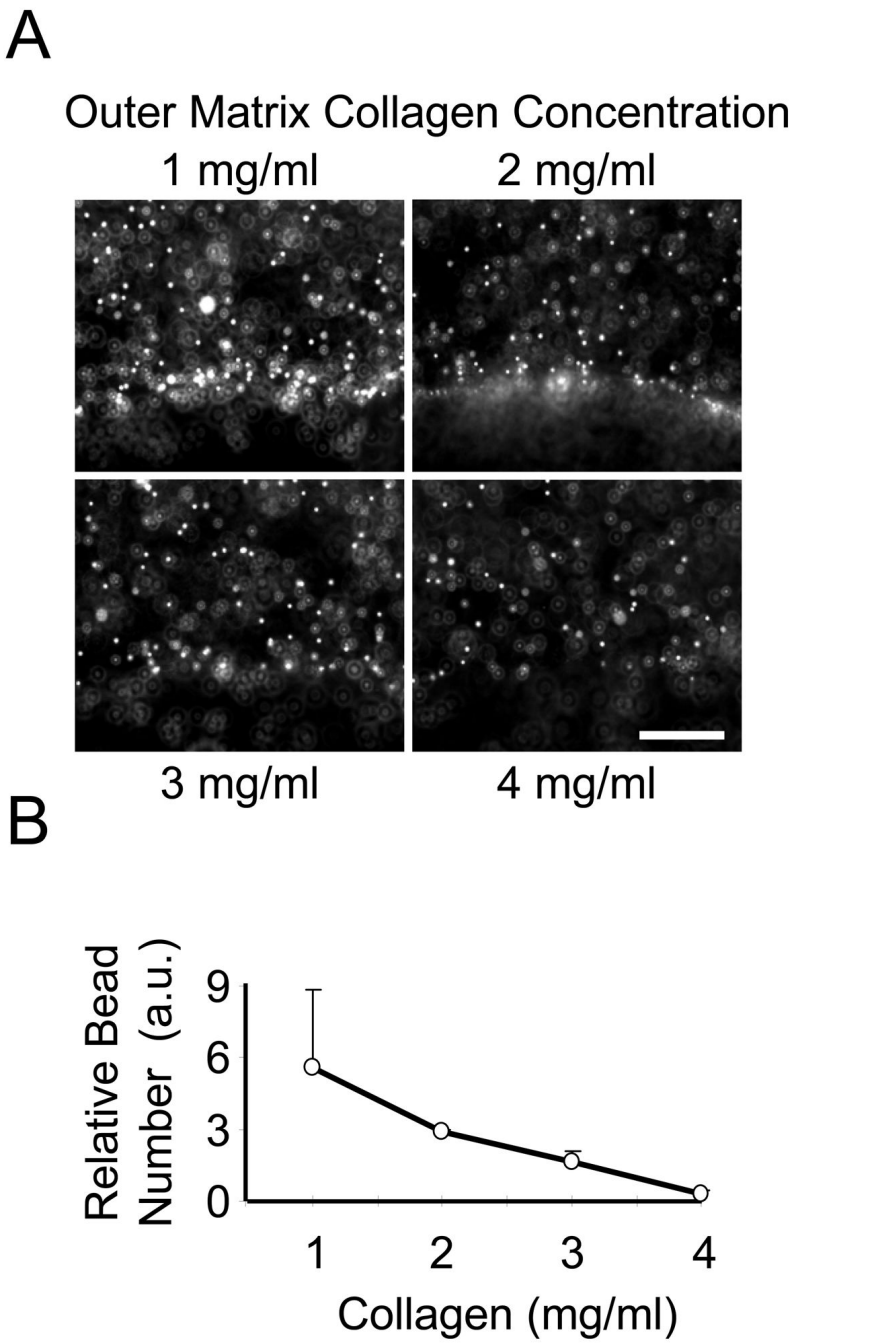

Figure 2. Collagen translocation in nested collagen matrices prepared with 1 to 4 mg/ml collagen outer matrices

(A) Floating nested matrices were incubated 24 h. Distribution of 6 μm fluorescent microspheres was visualized at the interface between inner and outer matrices. Bar = 200 μm. (B) Bead density at the interface was quantified using Image J software, and the extent of collagen translocation determined as bead # relative to starting conditions. Data shown are averages +/− SD based on two separate experiments with duplicate matrices for each collagen concentration. As the collagen density increased, collagen translocation decreased.

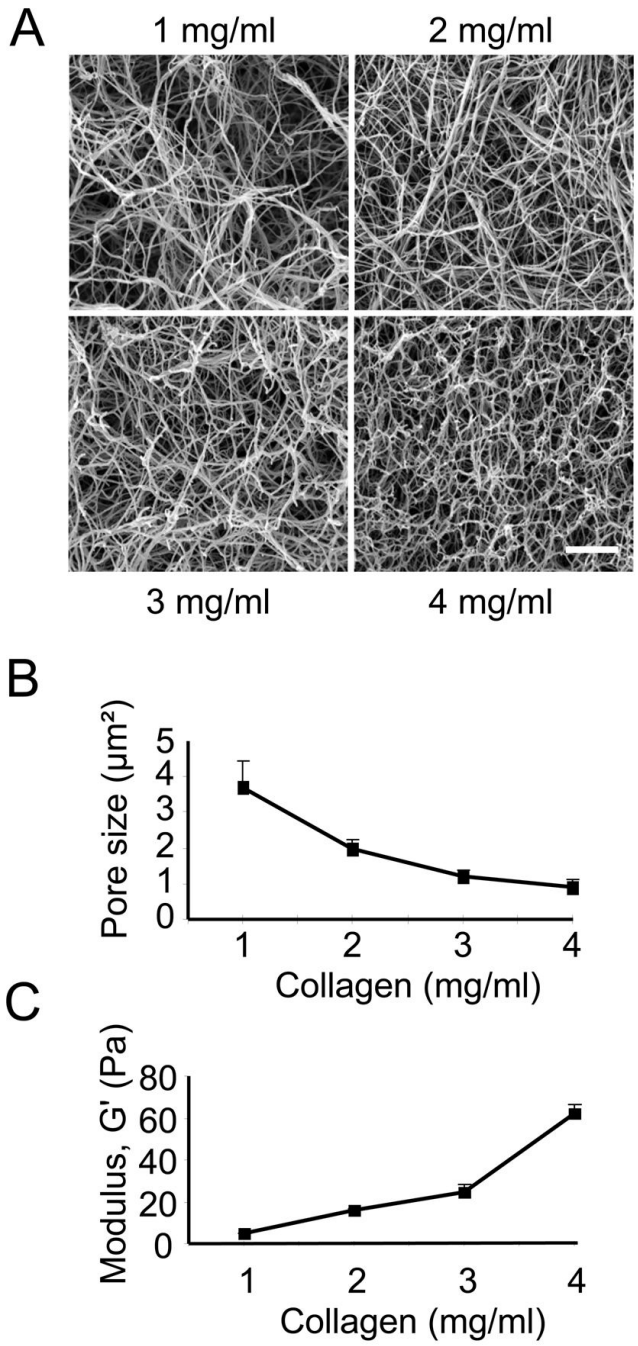

Figure 3. Quantitative measurements of porosity and stiffness of collagen matrices varying from 1 to 4 mg/ml collagen

Collagen matrices prepared at the collagen concentrations indicated were polymerized 1 h. (A) Samples that were fixed, critical point dried, and palladium coated were imaged by scanning electron microscopy. Bar = 5 μm. (B) Fibril spacing was quantified by measuring matrix poor size. Data shown are the averages +/− SD based on two separate experiments with duplicate matrices at each collagen concentration. (C) Freshly polymerized samples were used to measure matrix stiffness (storage modulus) by oscillating rheometry. Data shown are the averages +/− SD based on two separate experiments with triplicate matrices at each collagen

concentration. Increasing the collagen concentration resulted in decreased matrix porosity and increased matrix stiffness.

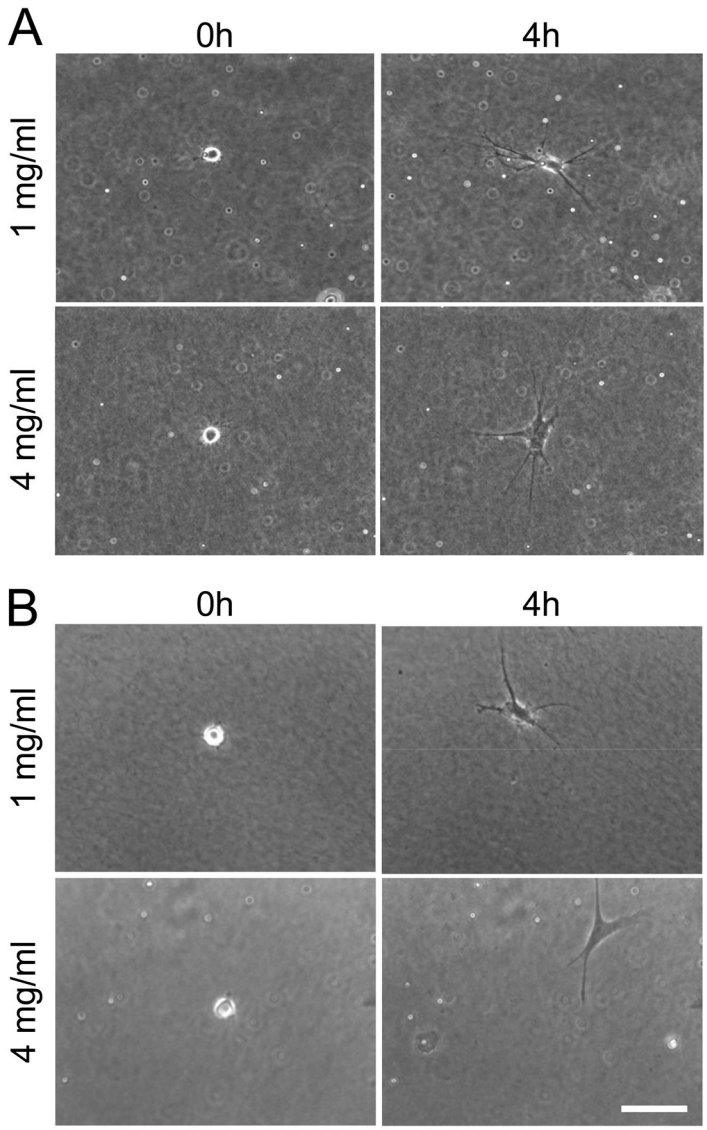

Figure 4. Motile activity of fibroblasts within and on top of collagen matrices

Phase-contrast images showing initial and final frames from time-lapse videos of fibroblasts incubated for 4 h (A) within (Supplemental time-lapse videos 1 and 2) and (B) on top of (Supplemental time-lapse videos 3 and 4) 1 and 4 mg/ml collagen matrices. Polystyrene beads (6 μm) added to the matrices were used to quantify collagen translocation. Bar = 100 μm. Cell spreading was dendritic within or on the surfaces of 1 mg/ml matrices. With 4 mg/ml matrices, cell spreading was dendritic within matrices but flattened and polarized on the surfaces of matrices, and cells on the surfaces of matrices began to migration.

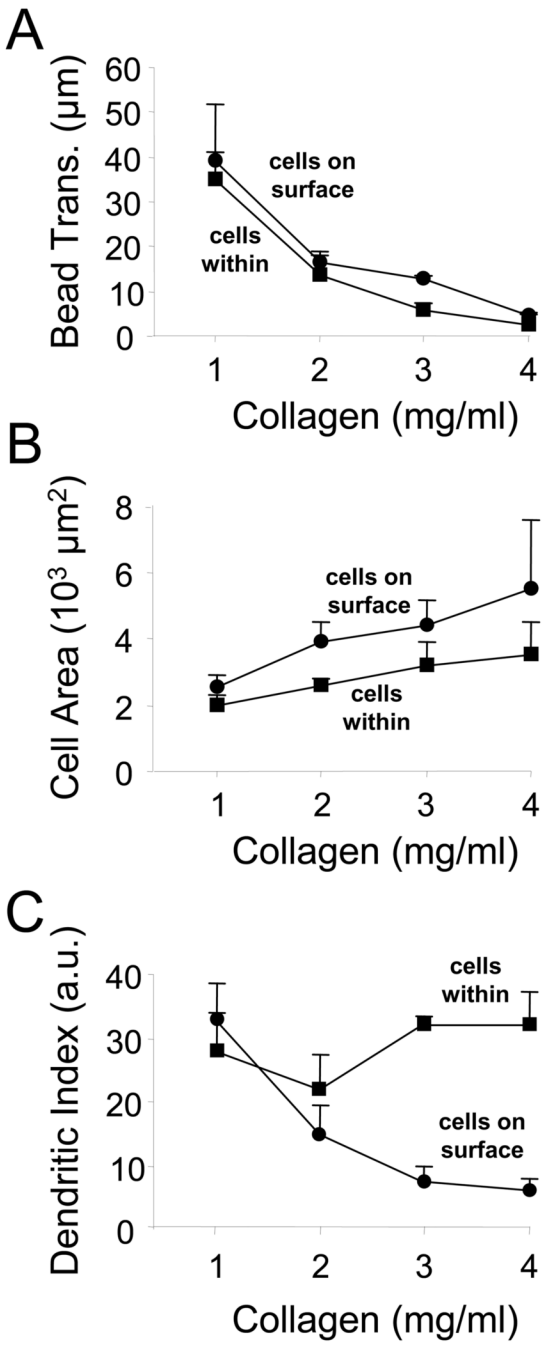

Figure 5. Collagen translocation and cell spreading of fibroblasts within and on top of collagen matrices

(A) Analysis of collagen translocation from time-lapse videos (Figure 4) as a function of collagen concentration based on displacement of 6 μm beads within the matrices. Data shown are the averages +/− SD based on three separate experiments. As the collagen density increased, collagen translocation decreased. (B & C) Fibroblasts were incubated 4 h within or on top of collagen matrices. At the end of the incubations, the cells were fixed and visualized by immunostaining for actin (c.f. Figure 6). Cell spreading (projected surface area) and cell shape (dendritic index) were determined by morphometric analysis. Data shown are the averages +/− SD of three separate experiments with five cells at each collagen concentration in each

experiment. As collagen concentration increased, the extent of cell spreading increased. Fibroblasts on top of matrices became more spread than cells within. Dendritic index was relatively constant for cells within matrices, but decreased as a function of collagen concentration for cells on top of matrices.

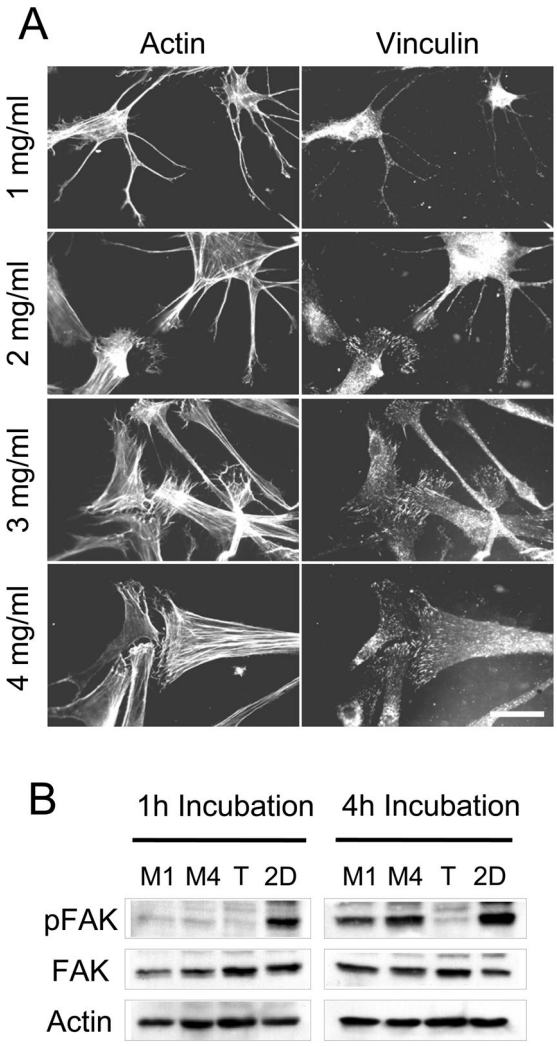

Figure 6. Actin stress fibers, focal adhesions, and focal adhesion kinase (FAK) Y397 phosphorylation by fibroblasts on top of collagen matrices

(A) Fibroblasts were incubated 4 h on top of collagen matrices prepared at the collagen concentrations indicated. At the end of the incubations, cells were fixed and visualized by immunostaining for actin and vinculin. As the collagen concentration increased, cell morphology switched from dendritic to flattened and polarized. Actin stress fibers (phalloidin staining) and focal adhesions (vinculin staining) were readily visible in the flattened cell regions. Bar = 50 μm. (B) Fibroblasts were incubated 1 and 4 h on top of collagen matrices prepared with 1 mg/ml collagen (M1) or 4 mg/ml collagen (M4) or on 50 μg/ml collagen-coated coverslips (2D). Cells incubated 1 h on collagen-coated coverslips but not on collagen matrices or trypsinized cells (T) showed FAK phosphorylation. After 4 h, fibroblasts incubated on collagen matrices also showed FAK phosphorylation. Data shown are representative of three independent experiments.

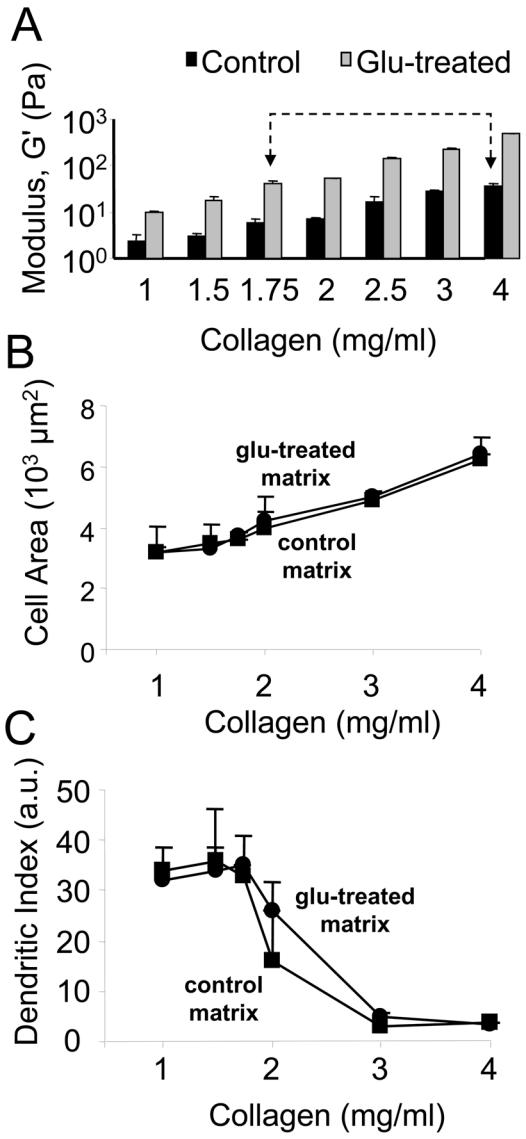

Figure 7. Cell spreading on collagen matrices stiffened chemically by treatment with glutaraldehyde

(A) Collagen matrices prepared with the collagen concentrations indicated were polymerized 1 h and then subjected to glutaraldehye (glu-treated) or PBS (control) treatment. Matrix stiffness (storage modulus) was measured by oscillating rheometry. Data shown are the averages +/− SD based on two separate experiments with triplicate matrices at each collagen concentration. Glu-treated samples had 5–10 fold increased matrix stiffness. (B&C) Fibroblasts were incubated 4 h on top of glu-treated and control matrices. At the end of the incubations, the cells were fixed and visualized by immunostaining for actin (c.f. Figure 8). Cell spreading (projected surface area) and cell shape (dendritic index) were determined by morphometric analysis. Data shown are the averages +/− SD of three separate experiments with five cells at each collagen concentration. Fibroblast spreading and dendritic index showed similar collagen concentration dependence regardless whether or not the matrices were stiffened by glu-treated.

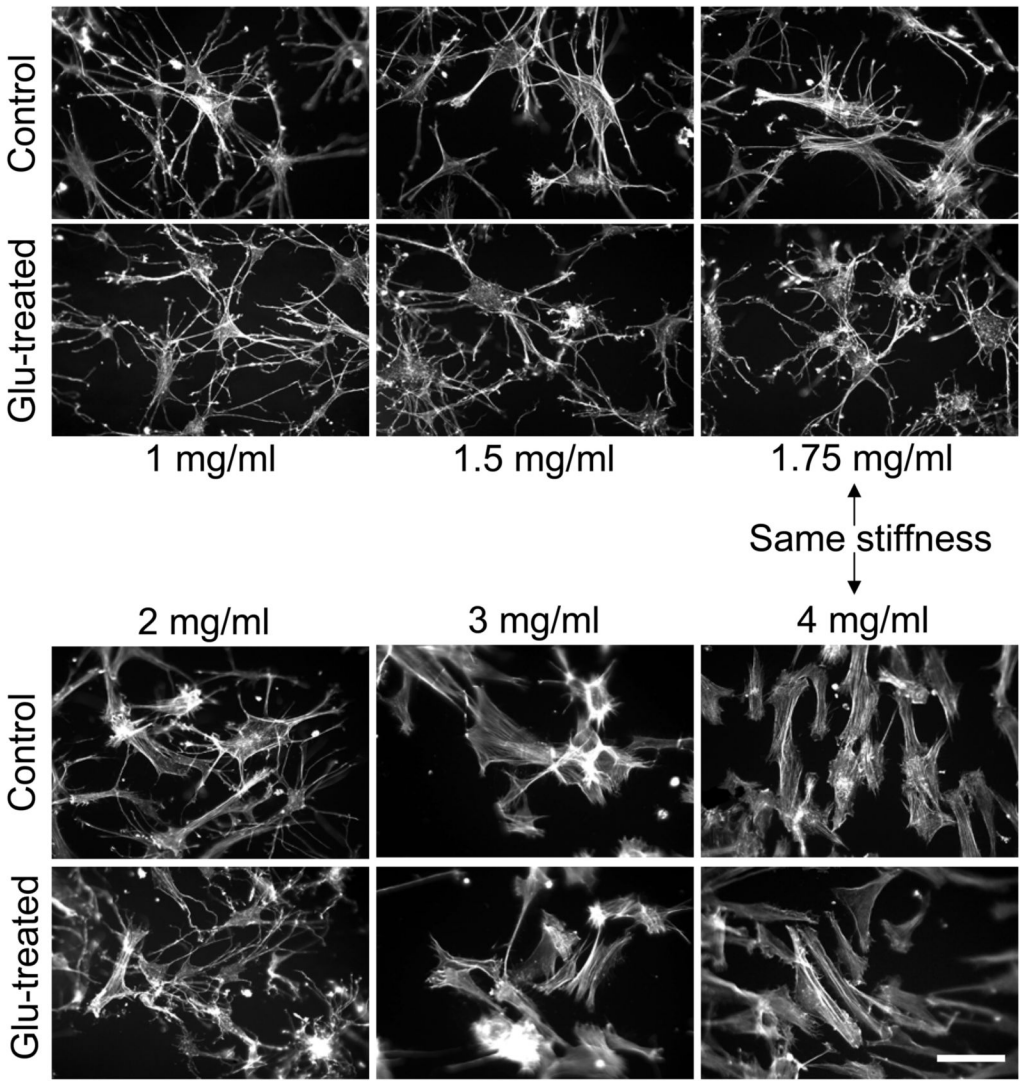

Figure 8. Cell morphology and actin stress fibers on collagen matrices stiffened chemically by treatment with glutaraldehyde

Fibroblasts were incubated 4 h on top of collagen matrices prepared at the collagen concentrations indicated and treated with or without glutaraldehyde as indicated in Figure 7A. At the end of the incubations, cells were visualized by immunostaining for actin. As the collagen concentration increased, cell morphology switched from dendritic to flattened and polarized and actin stress fibers were visible in the flattened cell regions. Increasing matrix stiffness by glu-treatment had no effect on cell morphological appearance. Bar = 50 μm.

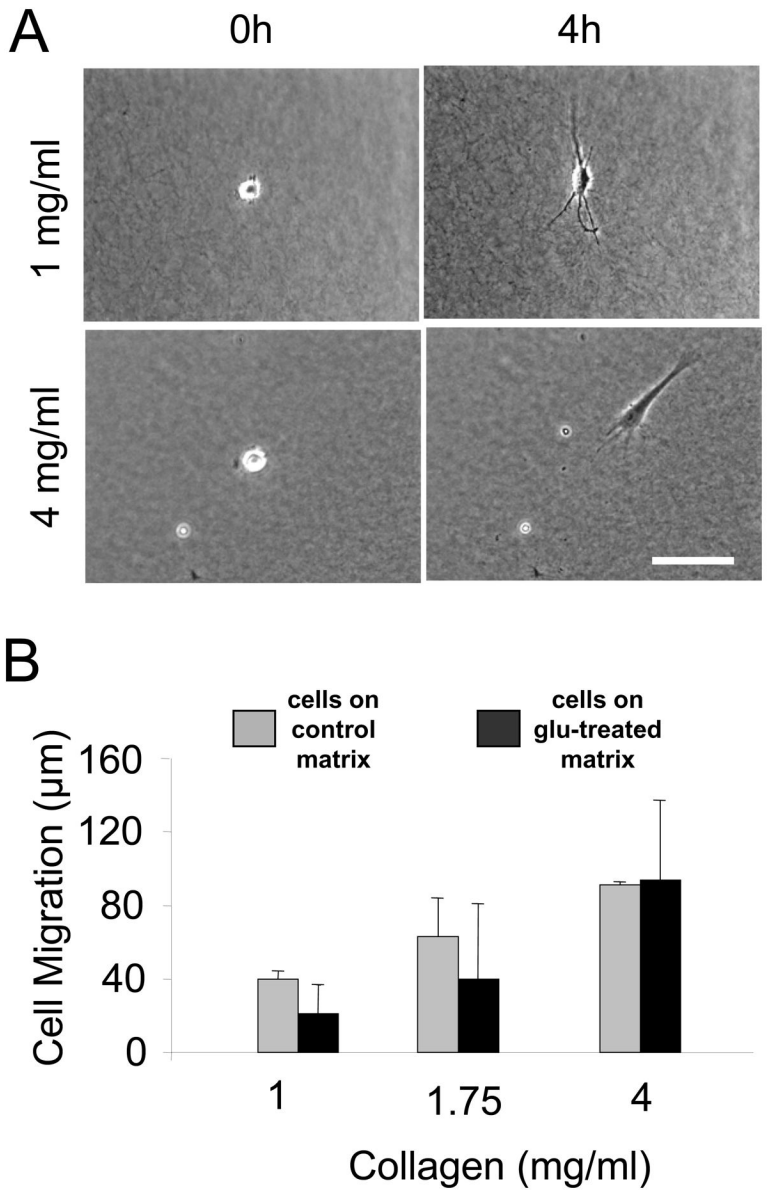

Figure 9. Cell migration on collagen matrices stiffened chemically by treatment with glutaraldehyde

(A) Phase-contrast images showing initial and final frames from time-lapse videos of fibroblasts incubated for 4 h on the surfaces of glu-treated (see Figure 7A) collagen matrices at the collagen concentrations indicated (Supplemental time-lapse videos 5 and 6). Cells on 4 mg/ml but not 1 mg/ml matrices developed flattened, polarized morphology and began to migrate. (B) Same as (A) except cell migration determined by measuring nuclear displacement. Data are the average +/− S.D of three separate experiments with five different cells for each collagen concentration. The extent of cell migration was similar on control and glu-treated matrices.